PHILOSOPHICAL TRANSACTIONS OF THE ROYAL SOCIETY A MATHEMATICAL, PHYSICAL & ENGINEERING SCIENCES

Plumbing Accretionary Prisms: Effects of Permeability Variations

J. Casey Moore, Kevin M. Brown, Frank Horath, Guy Cochrane, Mary MacKay and Greg Moore

Phil. Trans. R. Soc. Lond. A 1991 **335**, 275-288
doi: 10.1098/rsta.1991.0047

Plumbing accretionary prisms: effects of permeability variations

By J. Casey Moore[1], Kevin M. Brown[1], Frank Horath[1], Guy Cochrane[1], Mary MacKay[2] and Greg Moore[2]

[1] *Earth Sciences, University of California at Santa Cruz, California 95064, U.S.A.*
[2] *SOEST, University of Hawaii, Manoa, Honolulu, Hawaii 96822, U.S.A.*

Fault zones focus fluid expulsion in the muddy northern Barbados Ridge accretionary prism with fault-parallel permeabilities about 1000 times greater than intergranular permeabilities in the adjacent sediment. In the Oregon prism the low bedding-perpendicular permeability (due to mudstones) inhibits intergranular dewatering; however, intergranular flow is concentrated where submarine erosion breaches high permeability sandy layers. Even so, faults can capture fluid flow from these exposed sandy layers suggesting the faults have a still higher permeability. Such observations coupled with laboratory measurements permeabilities suggest that faults off Oregon may have fault-parallel permeabilities at least 10–10000 times greater than the adjacent sediments.

Results from Barbados and Oregon suggest fluid flow is concentrated along the most active faults. At the toe of prisms the fault zones are being progressively loaded by the thickening wedge and are undergoing compaction. Preliminary experiments show that permeability decreases relative to the surrounding wall rocks along faults within this compactive deformation régime; we believe that these faults must undergo dilation, perhaps linked to transient increases in pore pressure if they are to be preferential fluid conduits. Farther upslope erosion exposes rocks that are more consolidated, commonly more cemented, and generally of lower intergranular permeability than rocks of equivalent burial further seaward. Because of their lithification and overconsolidation these rocks dilate during faulting, locally enhancing fracture permeability. In such dilative régimes, faults become evermore focused zones of fluid expulsion relative to occluded intergranular pathways.

1. Introduction

Permeability is the most important factor controlling fluid flow in accretionary prisms. Fluid flow rate depends principally on permeability and hydraulic gradient. In accretionary prisms, permeability variations due to lithology can range over six to seven orders of magnitude (Horath 1989; Taylor & Leonard 1990); whereas, hydraulic gradients change by less than an order of magnitude (Moore & von Huene 1980); thus, permeability is at least one million times more variable than hydraulic gradient in governing fluid flow in accretionary prisms. In addition to its lithologic variability, permeability changes with structural evolution, diagenesis and metamorphism; permeability may also change during short-term deformational events on the timescale of the earthquake cycle (Sibson 1981).

Because fractures can radically affect permeability and accretionary prisms are highly faulted, large-scale field determination of permeability would be most

effective. Unfortunately such measurements have yet to be made; permeability data from accretionary prisms is limited to measurements from small samples. Inferences from these few data are based on geologic reasoning, experiments, and numerical modelling. Here we review information on the permeability structure of hydrogeologic end-members of accretionary prisms, present some new observational and preliminary experimental results, and attempt to conceptualize possible permeability variations in time and space.

We principally use units of m^2 for permeability but also scale diagrams in hydraulic conductivity with units of $cm\,s^{-1}$. Hydraulic conductivity is the proportionality constant in Darcy's law, sometimes erroneously referred to permeability; hydraulic conductivity equals the product of permeability, density, and the acceleration of gravity divided by viscosity (Freeze & Cherry 1979, p. 27). Equivalent permeability is used to describe an average or effective bulk measure of permeability in various lithologies or in various directions in units of anisotropic permeability structure (Freeze & Cherry 1979, pp. 32–34).

2. Permeability variation in muddy accretionary prism: Northern Barbados ridge

Long-distance lateral flow of fluids in subduction zones was first explicitly recognized through Ocean Drilling Program (ODP) investigations of the Northern Barbados Ridge (Moore *et al.* 1987, fig. 1). Here, the evidence for active fluid flow, principally along faults, is from geochemical (Gieskes *et al.* 1990) and temperature anomalies (Fisher & Hounslow 1990). These geochemical and temperature anomalies must be periodically replenished by fluid flow or they would be obliterated through diffusion. The geochemical and temperature data suggest fluid moves along the decollement zone with minor leakage into the imbricate thrusts, and negligible flow into the surrounding low permeability (Taylor & Leonard 1990), muddy sedimentary rock matrix (figure 1). Because the methane from the decollement zone has a thermogenic component, deep sources are necessary (Vrolijk *et al.* 1990). For fluids to be channelled for great distance along a fault zone and not be depleted by flow into the wall rocks, the fault zone permeabilities must be much higher than the wall rock. In the absence of *in situ* measurements, numerical models provide the only constraints on the relative magnitudes of wall rock and fault zone permeabilities.

To simulate the pore pressures of 60–100% of lithostatic near the base of the prism, the numerical model of Screaton *et al.* (1990) requires the overall equivalent permeability of the prism to lie between 10^{-16} and $10^{-18}\,m^2$ over the depth range penetrated by Site 671 of Leg 110. Because the permeability measurements on samples (Taylor & Leonard 1990) are so close to modelled equivalent permeability estimates, it appears that the permeability of the prism is relatively uniform and not controlled by fractures outside the local environment of certain of fault zones. To focus flow in the decollement the model of Screaton *et al.* requires that the decollement zone be at least three orders of magnitude more permeable than the overlying prim. Because an equivalent permeability of $10^{-14}\,m^2$ gives the most realistic values of the magnitude and distribution of pore pressure relative to the structure features, Screaton *et al.* believe this value is the most representative permeability for fluid flow along the decollement fault zone (figure 1). The decollement zone is described as having an equivalent permeability because the fluid

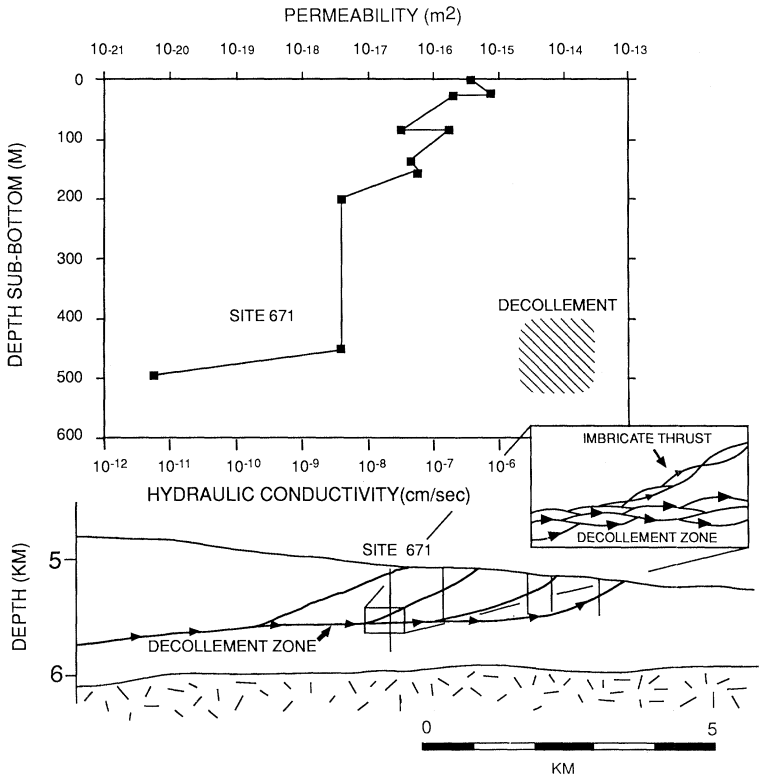

Figure 1. Permeability measurements for Site 671 penetrating the Northern Barbados Ridge (Taylor & Leonard 1990). Cross section and inset schematically depicts active fluid flow along decollement with minor leakage into imbricate thrust. Decollement zone permeability based on flow modelled parallel to this fault zone (Screaton *et al.* 1990).

would flow through both the intergranular matrix and fractures. The observation of veined fractures in fault zones from the Leg 110 area (Vrolijk & Shepard 1991) suggests that any significant permeability increase is due to dilation of fractures.

Overall Screaton *et al.* (1990) illustrate how powerful modelling can be in providing estimates of equivalent permeability and other types of data from the broad constraints of fluid pressure, flow paths, and prism geometry. Their particular approach involved steady-state deformation and fluid flow and hence inferences of permeability are time-averaged; episodic flow is likely and should be investigated through field monitoring and modelling.

3. Permeability variation in a sandy accretionary prism: Oregon margin

Although faults are important fluid conduits in muddy accretionary prisms, how important are faults in focusing fluid flow in sandy accretionary prisms, composed of thick sequences of siliclastic turbidites? Here, we review the observed flow paths and infer the permeability structure of the clastic-dominated Oregon margin. Individual permeability measurements are available from samples located with respect to structural features; seep distribution is established from more than 40 *Alvin* dives; the geometry of potential fluid conduits is constrained by an extensive multichannel seismic reflection grid.

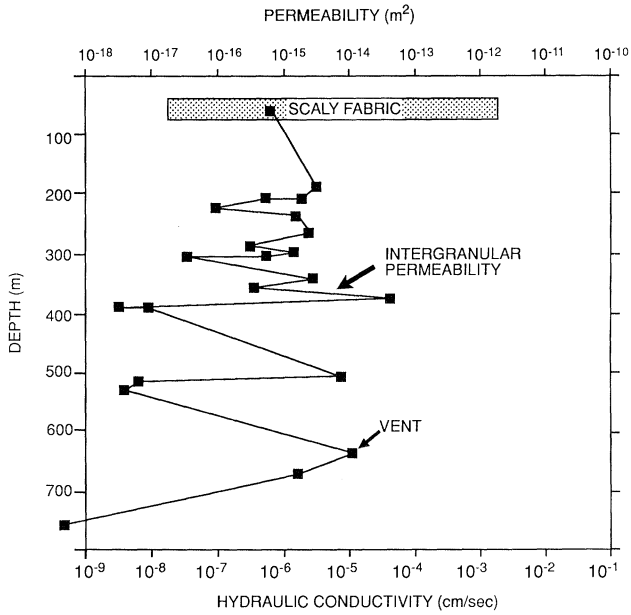

Figure 2. Permeability measurements from (1) submarine canyon exposure through ramp anticline at base of slope, Oregon subduction zone, and (2) related scaly fabrics from onshore fault zones (Horath 1989). Sample depth for intergranular permeabilities from Oregon margin is based on structural projection of samples to a single profile (figure 5*b*) with an allowance for erosion. Horizontal bar shows range of permeabilities from scaly fabrics from Neogene on-land exposures of the Cascadia accretionary prism. Burial depth for the scaly fabric measurements represents effective stress at measurement, assuming hydrostatic pressure. Higher values are for samples with the scaly fabric oriented parallel to flow direction; lower values are for samples with scaly fabric perpendicular to flow direction.

Intergranular permeability: directional heterogeneity

Permeability determinations were made on samples collected by *Alvin* from a submarine canyon exposure using a constant flow rate apparatus under isotropic confining stress of 0.3–0.6 MPa. Measurements of intergranular permeability (figure 2) were either measured at the effective stress of sampling (assuming hydrostatic pressure gradient) or restored to this pressure using various permeability-effective stress functions (Horath 1989). Because fluid pressures in the accretionary prism are likely to exceed hydrostatic, the reported permeabilities are minimum values.

A vertical permeability profile through a ramp anticline at the marginal ridge of the Oregon margin shows about four orders of magnitude variation in intergranular permeability, due to variations from the more muddy to the more sandy and silty lithologies (figure 2). This profile of intergranular permeabilities allows evaluation of the permeability of various structural features based on how they interact with the stratigraphic section. Equivalent permeabilities calculated for flow parallel and perpendicular to bedding (Freeze & Cherry 1979, p. 34) indicate a permeability of 3×10^{-15} m^2 along bedding surfaces and 7×10^{-18} m^2 across bedding surfaces. Thus, although sandy Oregon prism may have a higher mean intergranular permeability than the Northern Barbados Ridge, its large-scale equivalent permeability structure shows about a 400-fold anisotropy.

PHILOSOPHICAL TRANSACTIONS OF THE ROYAL SOCIETY A MATHEMATICAL, PHYSICAL & ENGINEERING SCIENCES

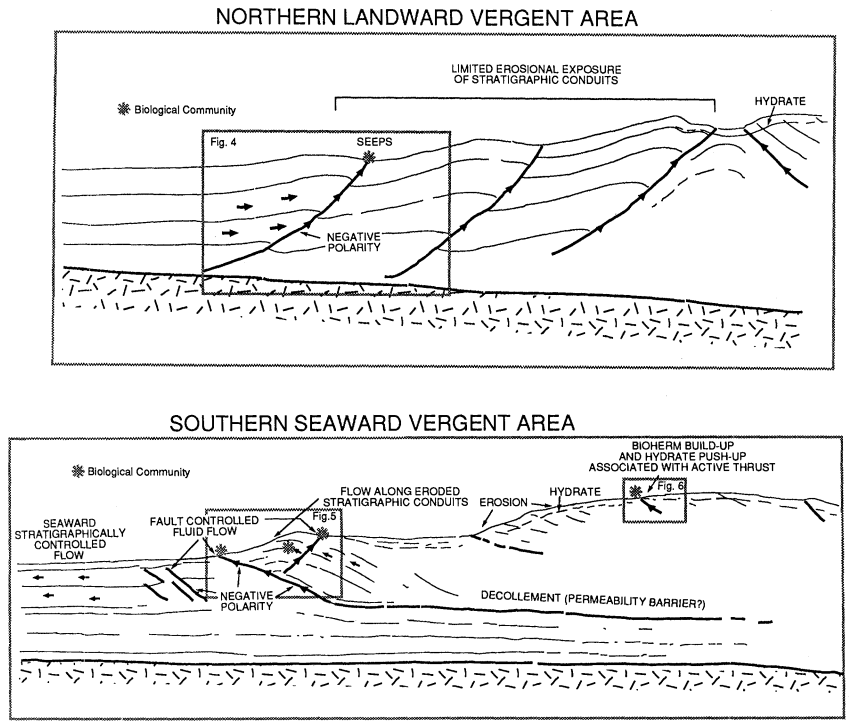

Figure 3. Generalized cross sections showing contrasting structural styles, geomorphic features, and seep geometries of northern landward and southern seaward vergent areas of Oregon margin.

Fluid flow paths in a faulted and uneroded stratigraphic section

In the landward vergent area offshore central Oregon minimal erosion has occurred off the hanging wall of the frontal thrust and the bedding parallel, high permeability conduits are not exposed. Flow to the surface must be either constrained to cut across bedding along flow paths with low equivalent permeabilities or to utilize faults (figures 3 and 4).

Biological evidence suggests the frontal thrust in the landward vergent area off Oregon is a conduit of fluid expulsion and therefore that it has significantly increased permeabilities. Concentrations of *Solemya sp.* clams suggest active flow along this fault zone (Kulm *et al.* 1986; Lewis & Cochrane 1990). The clam concentrations tend to occur in isolated groups along linear zones in a low area marking the surface intersection of the frontal thrust (figure 4).

The frontal thrust on seismic line OR-22 shows a high-amplitude, negative polarity reflection at about 1.75–2 s subbottom (about 2–2.5 km depth) (figure 4). We interpret this type of reflection as being due to a decrease in density and velocity in the fault zone due to an enhanced fluid content. The displacement along the fault is only in the region of a few hundred metres; this displacement, insufficient to cause an impedance contrast that would produce such a strong reflection, given the limited rate of change in density and velocity at this depth (Gregory 1977; Hamilton 1978). A reduced density in the fault zone is consistent with the fault zone having dilated during its formation (Gregory 1977). High fluid pressures developed as a consequence of rapid sediment accumulation in the fan sequence (Wang *et al.* 1990) many have contributed to this dilative behaviour.

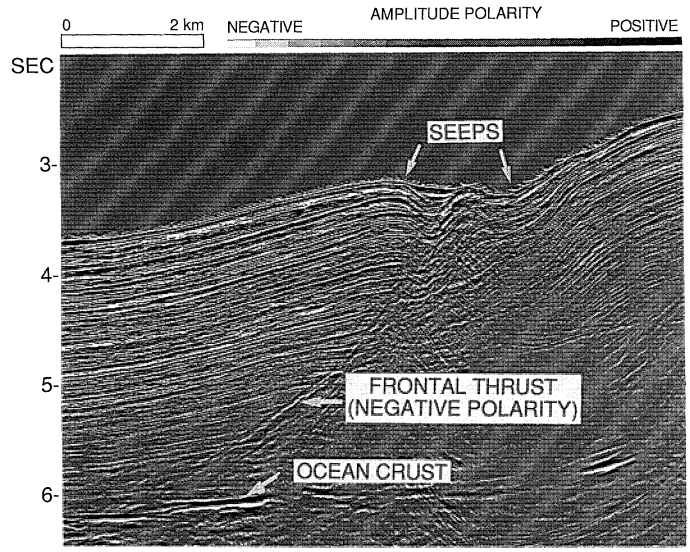

Figure 4. Detail of seismic reflection line OR-22 from deformation front of landward vergent region, Oregon subduction zone. Note the frontal thrust roots very near oceanic crust and shows a high-amplitude negative polarity reflection at depth. True amplitude display. Seep at surface marked by concentrations *Solemya* clams.

In the landward vergent area off Oregon faults apparently provide the highest permeability conduit for fluid expulsion. The existence of overpressures of depositional origin combined with any loading of the footwall due to overthrusting provides the pressure gradient to drive flow. The permeability of the fault must be higher than that of the equivalent permeability for flow perpendicular to the stratigraphic section or higher than about 10^{-17} m^2.

Exposed stratigraphic conduits and faults: seaward vergent area

In the southern part of the Oregon margin survey area, seaward verging structures have developed seaward facing erosional scarps, commonly on hanging walls of thrusts. Erosion cuts through sections of interbedded mudstone and sandstone-siltstone. Biological communities, marking vents, occur in the sandier and siltier layers at the crest of the breached anticlines indicating stratigraphic control on vent location (Moore *et al.* 1990). Concretions are common near the biological communities providing additional evidence for enhanced fluid flow. The single permeability measurement from one of the vent sites is amongst the highest measured from any of the sandy and silty lithologies (figure 2). The pressure gradient for fluid flow up landward tilted layers is caused by thrust imbrication (Wang *et al.* 1990).

The ramp anticline underlying the marginal ridge off Oregon is cut by a back thrust demarked by surface vents (Moore *et al.* 1990). Excepting the seep at the crest of the breached anticline, biological communities were not observed on the exposed bedding outcrops in a large submarine canyon up dip of the regions in which the back thrust is developed. Thus, this fault must either seal and/or capture lateral flow. Because the biological communities above the backthrust are more vigorous than those associated with the stratigraphic vents, we believe that flow is substantially captured due to a significantly higher permeability in the fault zone. A high permeability for scaly fabrics from fault zones supports this supposition (figure 2).

PHILOSOPHICAL TRANSACTIONS OF THE ROYAL SOCIETY A MATHEMATICAL, PHYSICAL & ENGINEERING SCIENCES

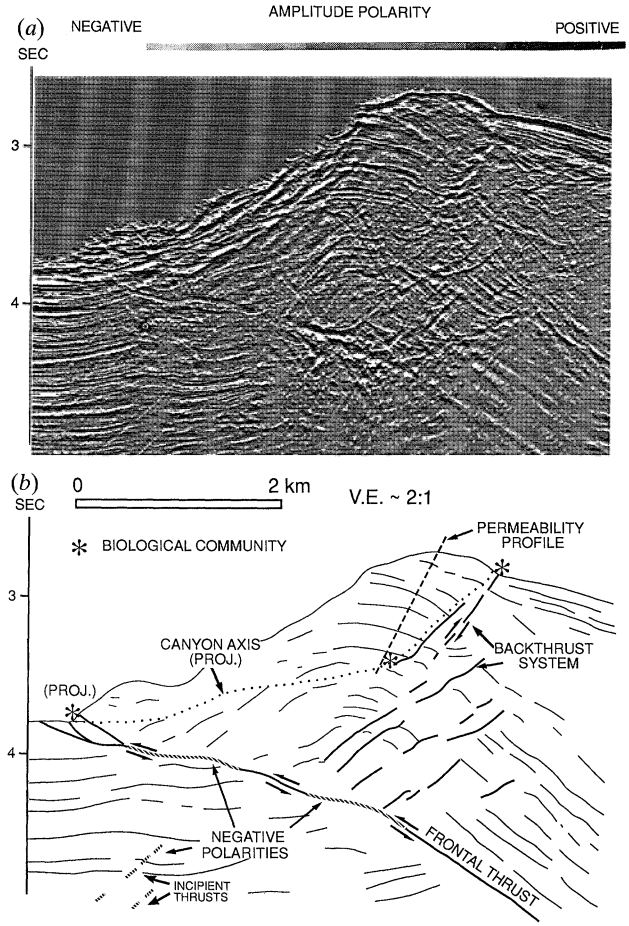

Figure 5. (*a*) Detail of seismic reflection line OR-9 from deformation front of seaward vergent area, Oregon subduction zone. True amplitude display. (*b*) Line drawing of line OR-9. Note regions of high-amplitude negative polarity reflections, associated with faults. Submarine canyon cuts ramp anticline along strike and allowed sampling and structural measurements within interior of fold. Canyon axis is projected from 1 to 2 km north. Biological community marking seep at frontal thrust is projected from 3 km to south.

Minor thrusts beneath the frontal thrust zone of the ramp anticline show amplitude anomalies with negative polarities (figure 5). These anomalies are unlikely to be due to displacement of rocks of significantly differing impedance, and probably result from fluid-rich low-density–low-velocity fault zones. Significant amplitude anomalies of negative polarity are also observed along the frontal thrust. The displacement on this fault is more than 1 km and may juxtapose sedimentary rocks of differing physical properties, creating the amplitude anomalies. In this area, however, a total of eight lines cross the frontal thrust, all with similar displacement but differing patterns of amplitude anomalies. The anomalies may be in part due juxtaposition of rocks of originally differing burial depths, but dilation along the fault zone is probably an important factor. The decreasing amplitude anomaly up the fault dip (figure 5) may be due to collapse of the fault resulting from lateral leakage of fluid to layers that are exposed in the canyon. This leakage also may explain *Alvin*

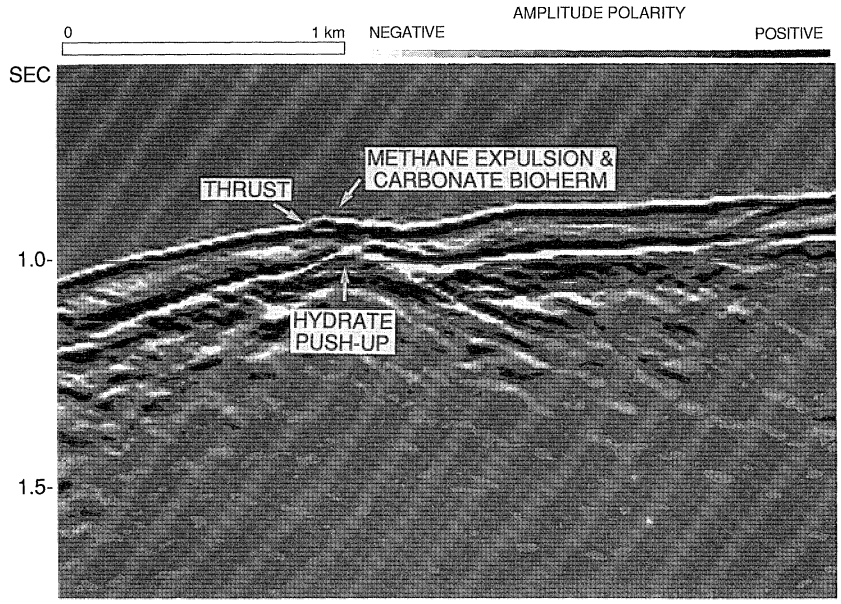

Figure 6. Detail of seismic reflection line OR-9 (see figure 3 for location). True amplitude display. Hyrate reflector is first prominent negative polarity reflector below water bottom. Hydrate reflector rises beneath trace of landward dipping thrust fault and is interpreted as being pushed up by flow of warm fluids. Submersible observations indicate active methane venting at surface and carbonate build-ups of *Calyptogena* clams and inorganically precipitated carbonate.

observations indicating a lack of vents up dip from the negative polarity anomaly on the seismic line in figure 5, but the presence of vents at the frontal thrust 3 km to the south where erosion of the ramp anticline is less severe.

Upslope venting and permeability evolution off Oregon

The evidence for continuing fluid seeps is apparent off Oregon both at a midslope level and beyond to shelf depths (Kulm & Suess 1990). In the region with seaward vergent structures discussed above, the midslope region is characterized by late thrusts that cut a large bathymetric high. One of these faults shows an upward deflection in the gas hydrate reflector that could be caused by enhanced flow and locally higher geothermal gradient (figure 6). Recent submersible observations at the surface trace of this fault indicate that it is venting methane bubbles, and that it supports the most concentrated chemosynthetic biological community yet seen off Oregon. Precipitation and biological action has led to the build up of a carbonate ridge many metres high. The focused flow indicates a substantial permeability contrast between the country rock and the fault zone in this region of the prism. One measurement of permeability from a cemented sandstone in this midslope here is 10^{-18} m^2. Because the faults are cutting cemented and substantially consolidated rocks, deformation would be dilatant with permeability enhancement in fault zones.

Discussion of Oregon accretionary prism observations

Faults that transmit fluids up through uneroded sections must have minimum permeabilities larger than the equivalent permeability necessary for flow perpendicular to the layering which corresponds to values greater than 10^{-16}–10^{-17} m^2. Apparently some faults have a higher permeability along their extent than the more

PHILOSOPHICAL TRANSACTIONS OF THE ROYAL SOCIETY A MATHEMATICAL, PHYSICAL & ENGINEERING SCIENCES

permeable sandy layers (greater than 10^{-13}–10^{-14} m^2), because these faults can capture flow from the sandy layers.

Although no fault zone material was collected during the *Alvin* program off Oregon, measurements of Neogene on-land equivalents suggest permeability values as high as 10^{-12} m^2 along scaly fabrics of faults and as low as 10^{-16}–10^{-17} m^2 across the scaly fabric of the fault rock (Horath 1989). Even though the sample scale is an order of magnitude greater than the mean fracture spacing, the measurements probably are minimum values (Sowers 1981); Because the measurements were made at confining pressures of 0.3–0.6 MPa and we have no applicable permeability-depth function, the measurements can only be compared with intergranular permeability measurements from shallow depths or low effective stresses. Nevertheless, the measurements indicate high permeabilities along flow paths parallel to the scaly fabric, permeabilities that would be sufficient to capture flow from the stratigraphic section at under low effective stress conditions. Moreover, modelling of the fluid expulsion off Oregon using Horath's (1989) values for intergranular permeability and fault permeabilities reproduce the observed flow paths well (Henry & Wang 1991).

4. Inferences on evolution and transience of permeability in accretionary prisms

Results outlined above from the Barbados Ridge and oregon accretionary prisms indicate that some faults, particularly active ones, localize fluid flow. However, not all faults encountered during Barbados ODP drilling conduct fluid preferentially. Apparently any permeability enhancement of fault zones is governed by the stress path of the fault zone material and cementation.

The compactive path: permeability evolution of faults being progressively loaded in a thickening wedge

Where erosion at the surface of the prism is minimal, most entering sediments will follow trajectories where they become progressively buried by sedimentary and tectonic thickening. We would expect these sediments, in both the wall rocks and fault zones, to compact (Karig 1986; Taylor & Leonard 1990). As permeability is strongly dependent on the number and degree of interconnection between pore voids (Freeze & Cherry 1979), higher degrees of compaction in fault zones (Atkinson & Bransby 1978; Karig 1986) should result in fault permeabilities being reduced relative to the wall rocks; such faults should not form fluid conduits.

Preliminary experimental results support the hypothesis that faults undergoing compaction and failure will have reduced fault-parallel permeabilities, in comparison with adjacent wall-rock (Brown & Moore 1990). In these experiments a mud sample (50% quartz, 30% illite, and 20% montmorillonite) 3 mm thick was placed along a 30° saw cut in a jacketed sliding block with permeability and diffusivity measured by a pulse test (Morin & Olsen 1987) along a flow path parallel to the sample extent. The deformation of the sample was incrementally stopped for permeability and diffusivity measurements. The axial load and confining pressure remained constant at 0.6 MPa during the permeability determinations so that the stress conditions correspond closely to the points on the failure curve (figure 7).

Our experiments suggest that faults deforming under compactive stress conditions will not increase in permeability but instead will become aquitards. As active faults in accretionary prisms can transmit fluids for at least portions of their histories, we

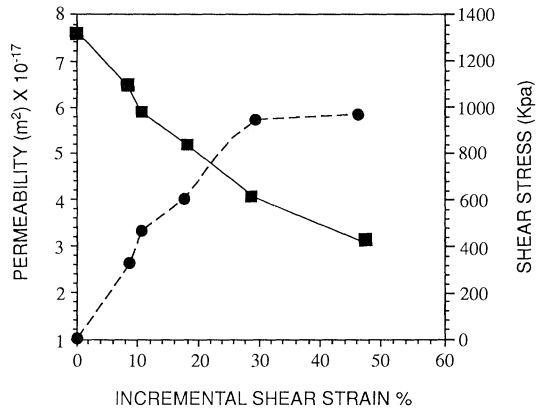

Figure 7. Permeability against shear strain and shear stress (o_1–o_3) against strain curves. Shear strain equals displacement divided by shear zone thickness. The progressive decrease in shear zone thickness (due to compaction) is accounted for in both the permeability and shear strain determinations. ■, Permeability; ●, failure curve.

believe that at these times these faults are not undergoing compactive failure but are dilated. The correlation of active venting with the apparently dilated faults associated with the negative polarity anomalies off Oregon (figures 4 and 5) supports this view. Moreover, Karig (1990) has argued for intermittent dilative deformation and high fluid pressure to account for the development of scaly fabrics in accretionary fault zones otherwise on a compactive strain path. Such a deformation scheme would also permit intermittent fluid flow.

In contrast to our experimental results, Arch & Maltman (1990) found that permeability increased parallel to shear zones in muddy sediments. However, their permeability measurements were made after unloading of the sample, reducing the effective stress to zero. The increased permeability is explicable by sample dilation. A combined interpretation of the experimental results of Brown & Moore (1990) and Arch & Maltman (1990) suggests that faults in unlithified sediments can only become fluid conduits when failure occurs under episodically reduced effective stresses conditions (figure 8). Increased fault-parallel permeabilities are probably associated with mechanical dilation of the sediments, probably along weak failure surfaces; typical fault-parallel orientation of the dilated failure surfaces leads to the focusing of flow along the fault plane. Arch & Maltman (1990) showed that the clay fabric alignment does produce a secondary anisotropy in permeability that would also assist in the channelling of flow along the fault zone.

The dilative path: permeability evolution during erosion

Significant mass wasting is common on the slopes of accretionary prisms (figures 3 and 9). Sediments uplifted and unloaded by erosion or faulting (Platt 1986) will tend to be overconsolidated and better lithified than sediments at equivalent depth in uneroded sections. Due to the overconsolidated and cemented nature of the sediments, regions undergoing active deformation will dilate (Atkinson & Bransby 1978) and increase in permeability. Undeformed regions will retain their low permeabilities. In active accretionary prisms, sites of significant erosion will always tend to be associated with active deformation because the prism equilibrium requires the erosion to be balanced by a similar amount of uplift (Davis *et al.* 1983). In the

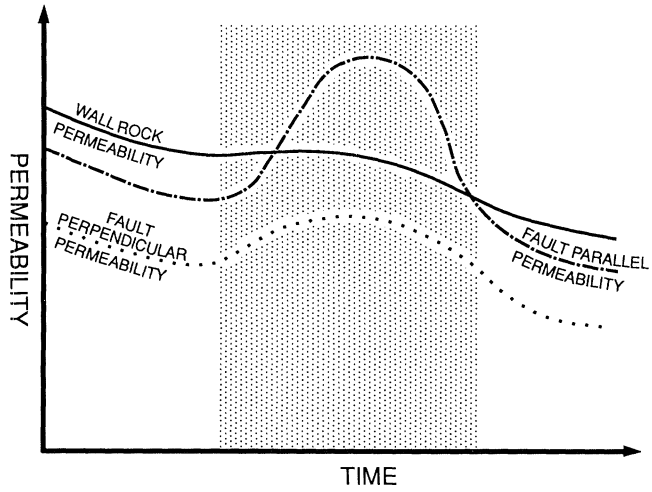

Figure 8. Conceptual evolution of fault permeability during compactive loading. Relative permeability trajectories of a segment of fault zone and the surrounding wall rocks at similar depths as they are progressively loaded during thrusting. Permeabilities in the fault zone are anisotropic but generally below the wall rock permeabilities during periods when the effective confining stresses are high. Transiently raised pore fluid pressures result in the episodic dilation of the shear surfaces and the fault parallel permeability exceeds the wall rock permeabilities. The higher fault-parallel permeabilities allow the excess pore pressure to diffuse along the fault zone and propagate fluid flow and displacement. Drainage of excess pressures results fracture closure and fault sealing. Stipple represents dilation and elevated pore pressure.

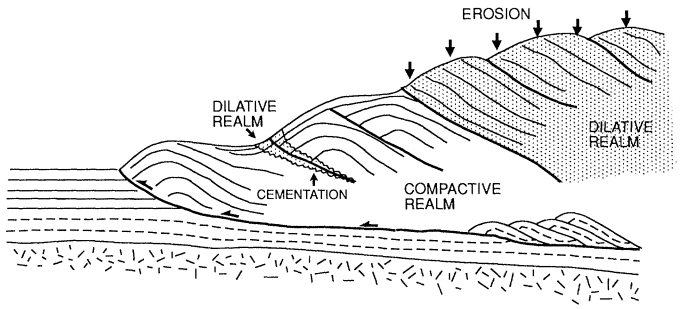

Figure 9. Schematic depiction of compactive and dilative realms of potential deformation in an accretionary prism. In the compactive realm sediments are under to normally consolidated, generally undergoing burial, and would suffer a decrease in volume and permeability during deformation. In the dilative realm sediments are over consolidated, due to erosion or cementation, and would increase in volume and permeability during deformation. In the generally compactive realm, fluid pressure transients could result in episodes of dilative deformation and permeability increase. As sediments are accreted and uplifted they would travel on deformation paths that are in general initially compactive (with possible dilative transients) followed by a generally dilative paths.

older regions of accretionary prisms, this uplift will commonly be accommodated on out-of-sequence thrusts; at the toe frontal imbricate thrusts produce the uplift. Because of the tendency of the uplifted rocks to dilate, these active structures in regions of erosion will become sights of considerable focused flow. For example, the active late thrust in the more interior regions of the Oregon prism is actively flowing fluid (figure 6).

Lithification, metamorphism, and permeability evolution

At deep levels in the prism (3–10 km burial) diagenesis and metamorphism apparently continue to reduce the intergranular permeability of low strain regions. Eventually only active deformation or hydrofracture development will allow further significant through-flow of fluid and the hydrogeologic system will become dominated by fracture flow (Vrolijk *et al.* 1988; Speed 1990). In addition crack seal textures and fluid inclusion studies (Vrolijk 1987; Fisher & Byrne 1990; Byrne & Fisher 1990), indicate that fluid flow in the deeper regions of accretionary prisms is associated with episodic phases of vein opening and mineral infilling. We would expect permeabilities of such fractured systems to fluctuate greatly with time.

5. Conclusions

1. Fault-parallel permeabilities in both in muddy and sandy accretionary prisms may be 1000 times higher than the average intergranular permeability of the adjacent sediment.

2. Transverse permeability in some fault zones may be as low as some of the lower permeability shales.

3. Sandy prisms vary in intergranular permeability over four orders of magnitude at a given depth of burial and show bulk anisotropy due to layering.

4. The more permeable layers in sandy accretionary prisms approach the fault-parallel permeability of the faults that actively leak fluid.

5. The magnitude of surface erosion and fault-sandy layer geometry significantly affects the geometry of fluid expulsion.

6. During compactive strain paths the permeability of fault zones generally decreases except during periods of dilative deformation, permeability increase, and fluid flow. During dilative strain paths, overconsolidation due to uplift and erosion, and cementation result in dilative deformation and permeability increase in fault zones; however, the adjacent wall rocks retain their low permeability caused by cementation and consolidation. Overall, a dilative strain path results in a more significant contrast between fault zone and wall rock permeability than a compactive strain path.

We thank the Royal Society for support to participate in the Discussion Meeting that fostered this paper. Research supported by NSF grants OCE-8609965, OCE-8912272, OCE-8813907, OCE-8917705 (tp C.M.) and OCE-8821577 (to G.M.). We thank Alex Maltman and Dave Prior for review of the typescript and John Tarney for editorial assistance.

References

Arch, J. & Maltman, A. 1990 Anisotropic permeability and tortuosity in deformed wet sediments. *J. geophys. Res.* **95**, 9035–9045.

Atkinson, J. H. & Bransby, P. L. 1978 *The mechanics of soils: an introduction to critical state soil mechanics*. London: McGraw-Hill.

Brown, K. M. & Moore, J. C. 1990 Deformation related permeability changes in muddy rocks. *Int. Conf. Fluids in Subduction Zones Abstr. vol.*, p. 27, Paris.

Byrne, T. & Fisher, D. 1990 Evidence for a weak and overpressured decollement beneath sediment-dominated accretionary prisms. *J. geophys. Res.* **95**, 9081–9097.

Davis, D., Suppe, J. & Dahlen, F. A. 1983 The mechanics of fold-and-thrust belts. *J. geophys. Res.* **88**, 1153–1172.

Fisher, D. & Byrne, T. 1990 The character and distribution of mineralized fractures in the Kodiak

Formation, Alaska: implications for fluid flow in an underthrust sequence. *J. geophys. Res.* **95**, 9069–9080.

Fisher, A. T. & Hounslow, M. 1990 Heat flow through the toe of the Barbados accretionary complex. In *Proc. Initial Reports* (*Part B*) *Ocean Drilling Project*, vol. 110, pp. 345–363.

Freeze, R. A. & Cherry, J. A. 1979 *Groundwater*. Englewood Cliffs, New Jersey: Prentice-Hall.

Gieskes, J. M., Vrolijk, P. & Blanc, G. 1990 Hydrogeochemistry of the Northern Barbados Accretionary complex transect: Ocean Drilling Project Leg 110. *J. geophys. Res.* **95**, 8809–8818.

Gregory, A. R. 1987 Aspects of rock physics from laboratory and log data that are important to seismic interpretation. In Seismic stratigraphy – applications to hydrocarbon exploration (ed. C. E. Payton). *Am. Ass. Petr. Geologists Mem.* **26**, 15–46.

Hamilton, E. L. 1978 Sound velocity-density relations in sea-floor sediments and rocks. *J. acoust. Soc. Am.* **63**, 366–377.

Henry, P. & Wang, C.-Y. 1991 Modeling of fluid flow and pore pressure at the toe of the Oregon and Barbados accretionary wedges. *J. geophys. Res.* (In the press.)

Horath, F. 1989 Permeability evolution in the Cascadia accretionary prism: examples from the Oregon prism and Olympic Peninsula melanges. M.Sc. thesis, University of California, Santa Cruz.

Karig, D. E. 1986 Physical properties and mechanical state of accreted sediments in the Nankai Trough, S. W. Japan. In Structural fabrics in Deep Sea Drilling Project cores from forearcs. *Geol. Soc. Am. Mem.* **166**, 117–133.

Karig, D. E. 1990 Experimental and observational constraints on the mechanical behavior in the toes of accretionary prisms. *Geol. Soc. Lond. Spec. Publ.* **54**, 383–398.

Kulm, L. D. & Suess, E. 1990 The relation of carbonate deposits to fluid venting processes: Oregon accretionary prism. *J. geophys. Res.* **95**, 8899–8915.

Kulm, L. D., Suess, E., Moore, J. C., Carson, B., Lewis, B. T., Ritger, S. D., Kadko, D. C., Thornberg, T. M., Embley, R. W., Rugh, W. D., Massoth, G. J., Langseth, M. G., Cochran, G. R. & Scamman, R. L. 1986 Oregon subduction zone: venting, fauna, and carbonates. *Science, Wash.* **231**, 561–566.

Lewis, B. T. R. & Cochrane, G. C. 1990 Relationship between chemosynthetic benthic communities and geologic structure on the Cascadia subduction zones. *J. geophys. Res.* **95**, 8783–8793.

Moore, J. C. & von Huene, R. 1980 Abnormal pore pressure and hole instability in forearc regions: a preliminary report. Ocean Margins Drilling Program, Washington, D.C.

Moore, J. C., Orange, D. L. & Kulm, L. D. 1991 Interrelationship of fluid venting and structural evolution, Oregon margin. *J. geophys. Res.* **95**, 8795–8808.

Moore, J. C. *et al.* 1987 Expulsion of fluids from depth along a subduction-zone decollement horizon. *Nature* **326**, 785–788.

Morin, R. H. & Olsen, H. W. 1987 Theoretical analysis of the transient pressure response from a constant flow rate hydraulic conductivity test. *Water Resources Res.* **23**, 1461–1470.

Platt, J. P. 1986 Dynamics of orogenic wedges and the uplift of high-pressure metamorphic rocks. *Geol. Soc. Am. Bull.* **97**, 1037–1053.

Screaton, E. J., Wuthrich, D. R. & Dreiss, S. J. 1990 Permeabilities, fluid pressures, and flow rates in the Barbados Ridge Complex. *J. geophys. Res.* **95**, 8997–9007.

Sibson, R. H. 1981 Fluid flow accompanying faulting: field evidence and models. In *Earthquake prediction: an international review*. American Geophysical Union, Maurice Ewing Series vol. 4, pp. 593–603.

Sowers, G. F. 1981 Rock permeability or hydraulic conductivity – an overview. In *Permeability and groundwater contaminant transport*. ASTM STP 746, pp. 65–83.

Speed, R. 1990 Volume loss and defluidization history of Barbados. *J. geophys. Res.* **95**, 8983–8996.

Taylor, E. & Leonard, J. 1990 Sediment consolidation and permeability at the Barbados forearc. In *Proc. Ocean Drilling Project, Scientific Results*, vol. 110, pp. 289–308.

Vrolijk, P. J. 1987 Tectonically-driven fluid flow in the Kodiak accretionary complex, Alaska. *Geology* **15**, 466–469.

PHILOSOPHICAL TRANSACTIONS OF THE ROYAL SOCIETY A MATHEMATICAL, PHYSICAL & ENGINEERING SCIENCES

Vrolijk, P. & Shepard, S. M. F. 1991 Syntectonic carbonate veins from the Barbados accretionary prism (ODP Leg 110) – record of paleohydrology. *Sedimentology*. (In the press.)

Vrolijk, P., Myers, G. & Moore, J. C. 1987 Warm fluid migration along tectonic melanges in the Kodiak accretionary complex, Alaska. *J. geophys. Res.* **93**, 10313–10324.

Vrolijk, P., Chambers, S., Gieskes, J. & O'Neil, J. 1990 Stable isotope ratios of interstitial fluids from the northern Barbados accretionary prism, ODP Leg 110. In *Proc. Ocean Drilling Program, Scientific Results*, vol. 110: College Station TX (Ocean Drilling Program), pp. 189–205.

Wang, C. Y., Shi, Y., Hwang, W. & Chen, H. 1990 Hydrologic processes in the Oregon–Washington accretionary complex – seaward vergent versus landward vergent margins. *J. geophys. Res.* **95**, 9009–9023.

PHILOSOPHICAL TRANSACTIONS OF THE ROYAL SOCIETY A MATHEMATICAL, PHYSICAL & ENGINEERING SCIENCES

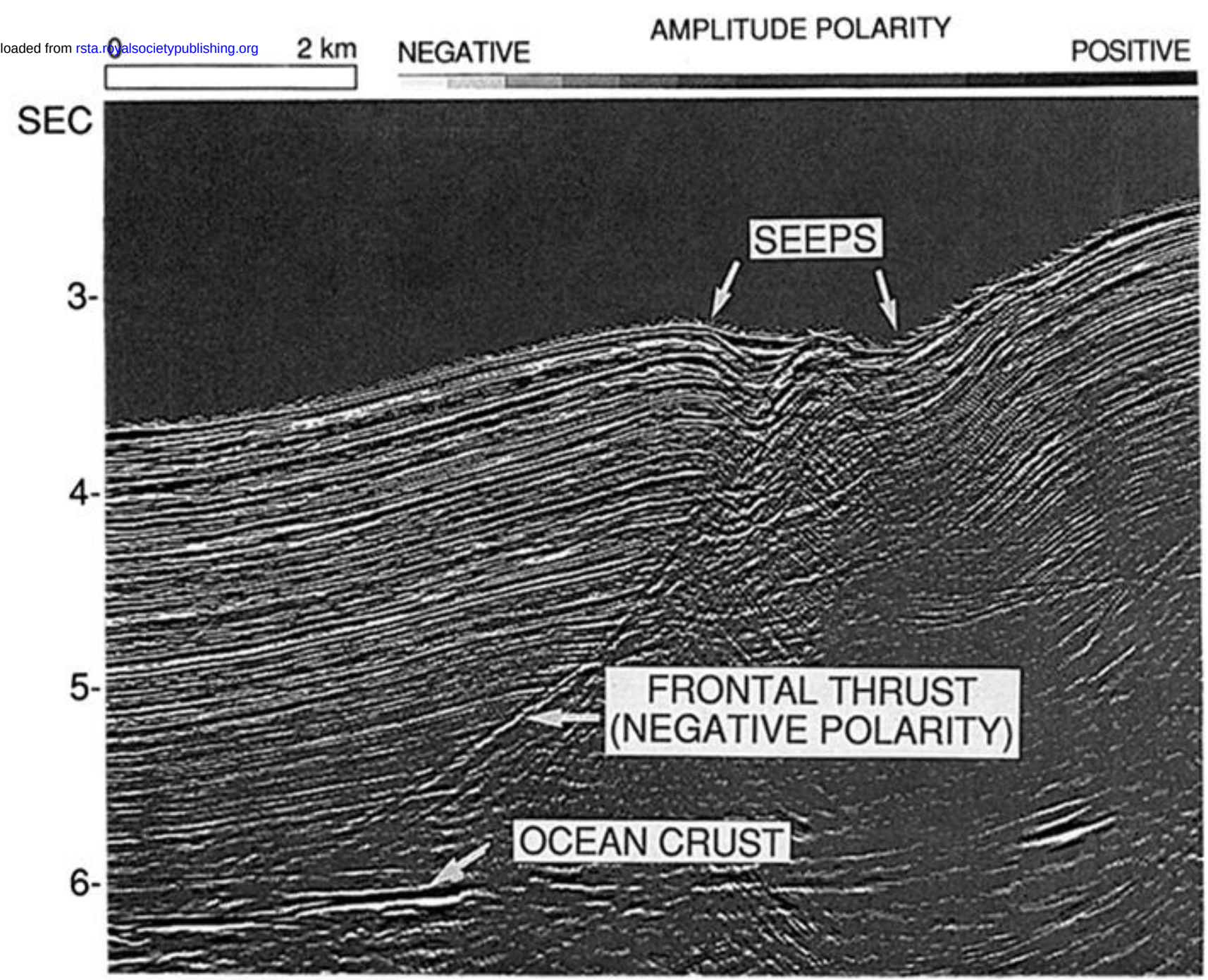

gure 4. Detail of seismic reflection line OR-22 from deformation front of landward vergent region, regon subduction zone. Note the frontal thrust roots very near oceanic crust and shows a high- nplitude negative polarity reflection at depth. True amplitude display. Seep at surface marked concentrations *Solemya* clams.

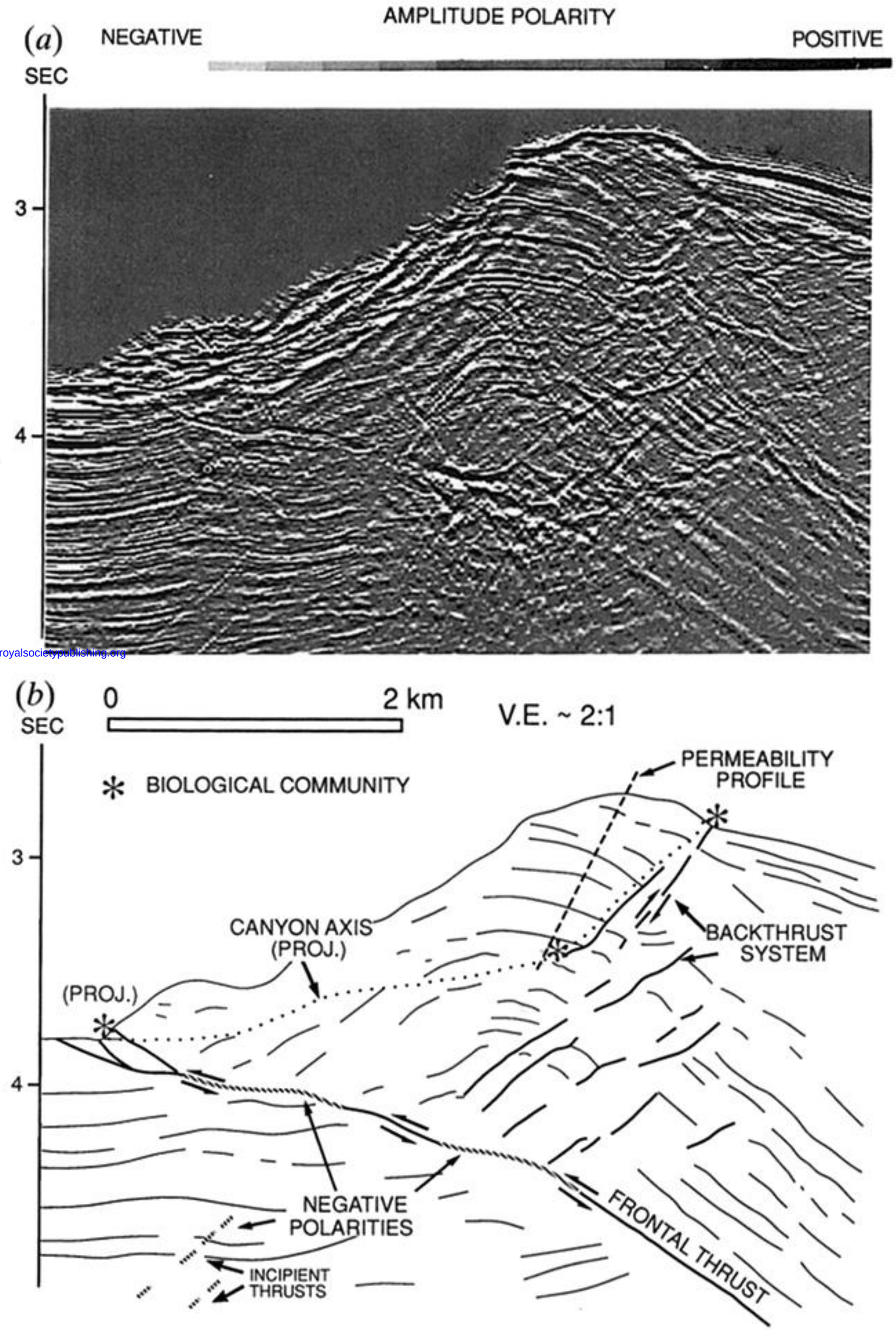

Figure 5. (*a*) Detail of seismic reflection line OR-9 from deformation front of seaward vergent area, Oregon subduction zone. True amplitude display. (*b*) Line drawing of line OR-9. Note regions of high-amplitude negative polarity reflections, associated with faults. Submarine canyon cuts ramp anticline along strike and allowed sampling and structural measurements within interior of fold. Canyon axis is projected from 1 to 2 km north. Biological community marking seep at frontal thrust is projected from 3 km to south.

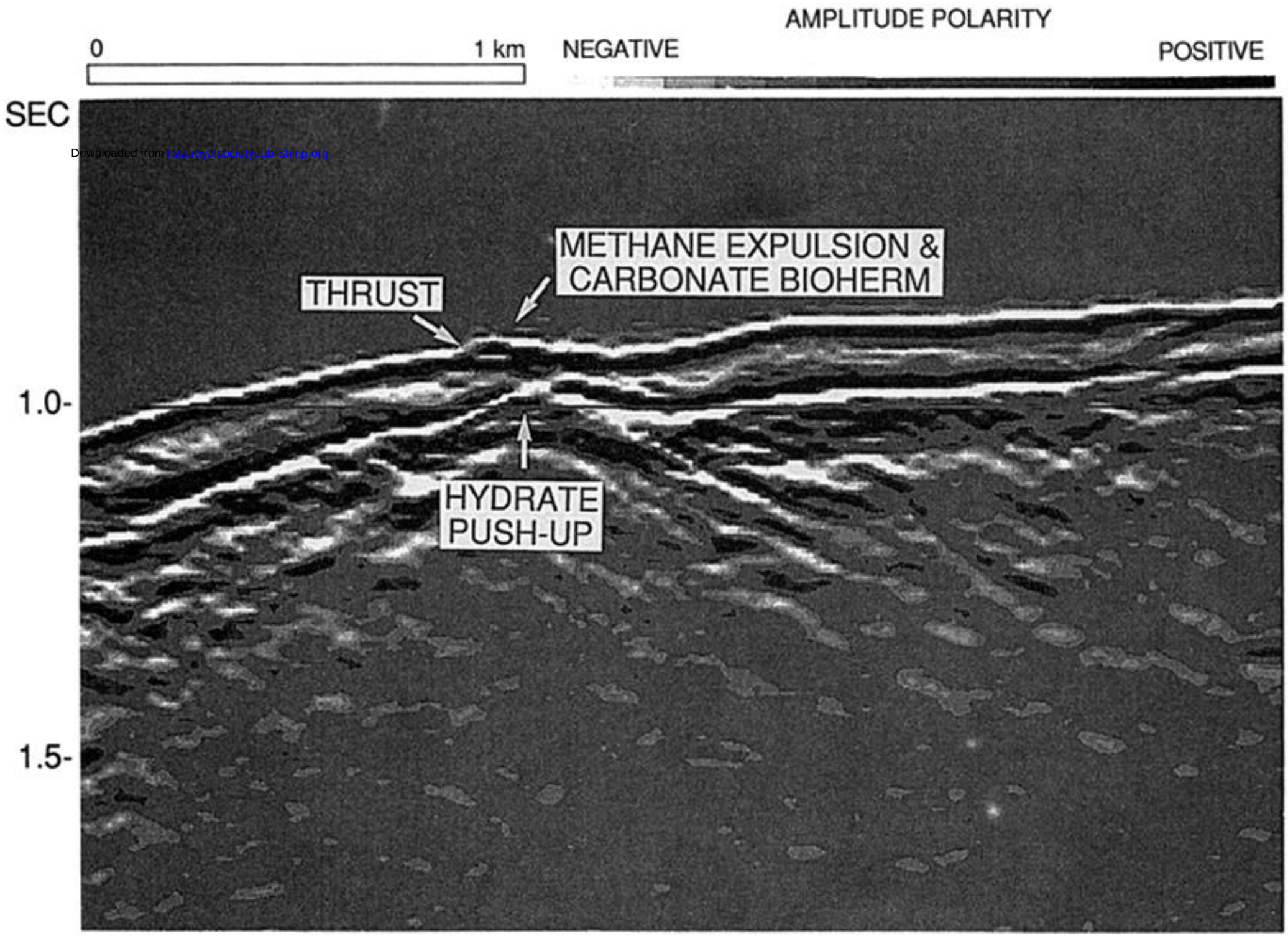

igure 6. Detail of seismic reflection line OR-9 (see figure 3 for location). True amplitude display. yrate reflector is first prominent negative polarity reflector below water bottom. Hydrate flector rises beneath trace of landward dipping thrust fault and is interpreted as being pushed up flow of warm fluids. Submersible observations indicate active methane venting at surface and rbonate build-ups of *Calyptogena* clams and inorganically precipitated carbonate.